ARTICLE

Color Purity in Polymer Electrochromic Window Devices on Indium–Tin Oxide and Single-Walled Carbon Nanotube Electrodes

Svetlana V. Vasilyeva,[†] Ece Unur,[†] Ryan M. Walczak,[†,§] Evan P. Donoghue,[‡] Andrew G. Rinzler,[‡] and John R. Reynolds*[,†]

The George and Josephine Butler Polymer Research Laboratory, Department of Chemistry, Center for Macromolecular Science and Engineering, and Department of Physics, University of Florida, Gainesville, Florida 32611-7200, and nRadiance LLC, 101 SE Second Place, Suite 201B, Gainesville, Florida 32601

ABSTRACT Dual polymer absorptive/transmissive electrochromic (EC) window devices have been assembled using the solution-processable and high-EC-contrast polymer PProDOT-$(CH_2OEtHx)_2$ as the EC material, along with a non-color-changing electroactive polymer, poly(2,2,6,6-tetramethylpiperidinyloxy-4-yl methacrylate) (PTMA), as the counter electrode material. Indium–tin oxide (ITO) and highly transmissive single-walled carbon nanotube (SWNT) film coated glass electrodes are used as electrode substrates. The use of the EC/non-color-changing polymer combination allowed us to construct window devices that rapidly switch between magenta and highly transmissive (>95% T for ITO and ~79% T for SWNT) states with large optical modulation (>71% ΔT for ITO and 66% ΔT for SWNT). The devices showed effective coloration and bleaching: the lightness parameter (L^*) changing from 67 to 95 for ITO (~50–92 for SWNT), essentially reaching a diffuse white upon oxidation. The color modulates from highly pure magenta with $a^* = 28$ (red hue) and $b^* = -28$ (blue chroma) for ITO ($a^* = 40$ and $b^* = -36$ for SWNT) to nearly colorless with $a^* = 1$ and $b^* = -1$ for ITO ($a^* = -2$ and $b^* = -3$ for SWNT) devices. Increasing the switching voltage from 2.55 V up to 3.5 V resulted in faster SWNT-based window device performance.

KEYWORDS: electrochromism • conjugated polymer • electrochromic device • single-walled carbon nanotube films

1. INTRODUCTION

Electrochromic (EC) materials undergo reversible color changes as a function of an externally applied voltage and have been extensively studied for a wide variety of EC device (ECD) applications, including smart windows for residential buildings, aircraft, and vehicles, vision systems, antiglare dimming mirrors (1–3), camouflage (4), electronic paper (5, 6), and nonemissive EC displays (7). Among the different types of EC materials, inorganic (transition-metal oxides (8–10) and mixed-valence metal complexes (11)), molecular organics (12), and conjugated polymers have gained considerable attention as prospective materials for ECD applications over the past decade (13–15). Their propensity for fine color-tuning via structural modification of the polymer backbone, intrinsic optical properties, ease of processability, and high stability upon multiple redox switching makes conjugated polymers promising candidates for display applications (16–18). Depending on its redox state, an EC material can exist in one or more absorptive *colored states* or one or more highly transmissive or completely colorless *bleached states*. Materials exhibiting a highly absorptive colored state and a completely colorless bleached state are the most desirable EC materials for most applications, especially displays and smart windows.

The most extensively studied dual polymer absorptive/transmissive, or window-type, ECD configuration consists of two facing transparent conducting electrodes coated with complementarily colored cathodically and anodically coloring EC polymers (19), separated by a thin layer of gel electrolyte to allow rapid switching of the device between colored (absorptive) and bleached (transmissive) states. The so-called cathodically coloring polymers have relatively low band gaps (on the order of 1.5–2.0 eV), giving them a strong π,π^* absorption in the visible region and a distinct color in the neutral state. Upon oxidation, the π,π^* absorption depletes and the polymer becomes highly transmissive as the light absorption is transferred to the near-infrared. Anodically coloring high-band-gap polymers exhibit opposite electrooptical properties: they are almost colorless and transparent in the neutral state and highly colored in the oxidized state because of a high band gap (typically above 3.0 eV) in the neutral state and a polaron/bipolaron absorbance in the visible region.

This type of device configuration has two major advantages. First, cathodically and anodically coloring polymers change their color states simultaneously: at one bias, the high absorbance of the device is due to both polymers being in their colored states, and upon reverse bias, both polymers are converted to their bleached states. As a result, an enhanced optical contrast of the device is expected. Second,

* Corresponding author. Phone: 352-392-9151. Fax: 352-392-9741. E-mail: reynolds@chem.ufl.edu.

Received for review June 23, 2009 and accepted August 15, 2009

[†] Department of Chemistry, Center for Macromolecular Science and Engineering, University of Florida.

[§] nRadiance LLC.

[‡] Department of Physics, University of Florida.

DOI: 10.1021/am900435j

© 2009 American Chemical Society

Published on Web 09/16/2009

the use of two redox-active materials allows balancing of the charge of the device, thus preventing undesired side reactions and ensuring improved lifetime characteristics. For example, window ECDs using solution-processable dialkyl-substituted poly(alkylenedioxythiophene) (PXDOT) derivatives, such as PProDOT-$(CH_2OC_{18}H_{37})_2$ and PProDOT-$(CH_2OEtHx)_2$ as cathodically coloring polymers, in conjunction with electrochemically deposited poly[3,6-bis(2,3-dihydrothieno[3,4-*b*][1,4]dioxin-5-yl)-9-methyl-9*H*-carbazole] (PBEDOT-NMeCz) as an anodically coloring polymer, yielded 45% and 77% luminance contrast, respectively, which is higher than the optical contrast of the individual EC polymers (22).

However, the combined residual absorbance of the two conjugated EC polymers in their bleached state colors what should be a clear state, limiting the maximal transmittance and thus reducing the overall contrast provided by the device. Moreover, the color purity induced in the absorptive state of the dual EC polymer systems is reduced because each polymer typically absorbs over a different wavelength profile. Systematic characterization of several dual EC polymer windows by Padilla et al. have demonstrated both theoretically and experimentally that, although some dual combinations exhibit enhanced optical contrast compared with the individual polymers (22), in the majority of cases, the maximum contrast achieved for a dual polymer combination is lower than that for one or the other of the constituent materials (20). It is important to emphasize that high transmittance is one of the most desirable features of any vision system because "smart" window ECDs should provide a full, unmitigated view of the environment.

To improve the optical contrast of the device, EC polymers with a very high transmittance in their bleached states could be used. As previously reported by our group, the use of highly transparent anodically coloring polymers, such as *N*-propane-sulfonated poly(3,4-propylenedioxypyrrole) (PProDOP-NPrS), in combination with a cathodically coloring PProDOT$(Me)_2$ polymer resulted in a ~15% increase in the contrast of the window ECD compared to devices containing the less transmissive PBEDOT-NMeCz polymer as the anodically coloring electroactive layer (21).

An alternative approach to achieving both enhanced transmittance and maximum contrast in a dual polymer window ECD is to utilize an especially high contrast EC polymer as the EC functional layer in conjunction with a *non-color-changing polymer* as an electroactive counter electrode, or an effective charge sink, for the EC polymer. This approach allows retention of a highly saturated (pure) and vibrant color of the EC polymer in the device, which is especially difficult to attain when using the combination of two EC polymers having different color hues.

Recently, Nishide et al. reported the application of organic polymers containing stable radical pendant groups, termed radical polymers, as electroactive and charge-storage materials for rechargeable batteries (23–27). Taking advantage of the excellent properties of these radical polymers, which includes reversible redox behavior, rapid electron transport, and the ability to form transparent electroactive films, they have also applied 2,2,6,6-tetramethylpiperidinoxyl (TEMPO)-substituted polymers as non-color-changing electroactive materials for the counter electrodes in ECDs (28, 29). ECDs using either Prussian blue (28) or the polyion complex of poly(decylviologen) and poly(styrenesulfonate) (PV10–PSS) (29) as EC materials in combination with the non-color-changing transparent TEMPO radical polymer operate at low driving voltages and demonstrate reversible charging/discharging behavior.

In this work, we report on our efforts to improve the window-type ECD performance by applying the TEMPO-substituted radical polymer poly(2,2,6,6-tetramethylpiperidinyloxy-4-yl methacrylate) (PTMA) as a transparent and colorless electroactive counter electrode in combination with a high-contrast, cathodically coloring polymer. In this instance, we have used PProDOT-$(CH_2OEtHx)_2$, which belongs to a large family of soluble alkyl- and alkoxy-substituted PXDOT derivatives developed and studied by our group (30–32). Exhibiting excellent transmittance in its bleached state, a high intrinsic optical contrast (56% luminance change), a rapid subsecond redox switching, and a brilliant pure magenta/purple color, PProDOT-$(CH_2OEtHx)_2$ is an excellent EC material for the working electrode (22).

In addition to the active materials, the transparent conducting electrode is an important component in attaining a desirable form factor for window-type ECDs. Traditionally, ECDs have relied on indium–tin oxide (ITO) on glass as the transparent electrode; however, ITO is disadvantageous because of its rapidly increasing price and intolerance toward bending on flexible substrates. Because many of the promising examples of ECDs are flexible and in many cases would be applied to large substrates, it is critical to find an alternative bendable and transparent electrode. While our group has demonstrated the use of the conjugated polymer PEDOT:PSS as a flexible electrode in an all-plastic ECD (3), switching times were long (on the order of tens of seconds) because of the high surface resistivity (~600 Ω/□) of PEDOT:PSS. Recently, single-walled carbon nanotube (SWNT) films have emerged to the forefront of research on transparent electrodes because of their high bending radius, environmentally friendly fabrication conditions, chemical inertness, and low surface resistivity (≤80 Ω/□) (33). Furthermore, the high surface area of SWNT films allows for extensive contact area between the carbon nanotubes and the EC polymer and thus potentially faster device operation. However, in contrast to the hydrophilic surface of ITO, the surface of SWNT films, which resemble the basal plane of graphite, is relatively low in energy and does not readily adhere molecules through hydrogen-bonding and/or coordinative interactions. Thus, polymer delamination is a problem. As a solution, we demonstrate a pyrene-functionalized polyfluorene, designated Sticky-PF, which strongly binds to SWNT side walls through van der Waals interactions and serves as a nanotube "surface primer", improving ECD function.

2. EXPERIMENTAL SECTION

2.1. Materials. Lithium perchlorate ($LiClO_4$), poly(methyl methacrylate) (PMMA; M_w = 996 000 g/mol), ferrocene (Fc), toluene, and ethylene carbonate (EC) were purchased from Aldrich and used as received. Tetra-*n*-butylammonium perchlorate (TBAP) was synthesized by the metathesis of tetra-*n*-butylammonium bromide (98%, Sigma-Aldrich) and concentrated perchloric acid (≥69%, Fluka). The product was then recrystallized three times from isopropyl alcohol and dried in a vacuum oven at 70 °C for 3 days. Propylene carbonate (PC; Sigma-Aldrich) and acetonitrile (ACN; Aldrich) were distilled and dried before use. Glass beads (100 μm) were obtained from BioSpec Products, Inc., washed with acetone, and dried in air. PProDOT-$(CH_2OEtHx)_2$ was synthesized according to the methodologies previously reported (31). Non-color-changing poly(2,2,6,6-tetramethylpiperidinyloxy-4-yl methacrylate) (PTMA) was provided by Ciba. The polymer films were spray-cast onto electrode plates using an airbrush (Iwata-eclipse HP-BS) at 20 psi argon pressure. PProDOT-$(CH_2OEtHx)_2$ was sprayed from a 2 mg/mL solution in toluene. Non-color-changing electroactive films were spray-cast from 1:4 (weight ratio) of a PTMA/PMMA mixture in toluene (a 15 mg of PTMA/60 mg of PMMA/60 mL of toluene solution) and annealed for 40 min at 85 °C in a vacuum oven before characterization. All polymer solutions were filtered through 0.45 μm Whatman Teflon [poly(tetrafluoroethylene)] syringe filters prior to spraying. ITO-coated polished float glass slides CG-51IN-CUV (7 × 50 × 0.7 mm, R_s = 8−12 Ω/□) and CG-51IN-S107 (25 × 75 × 0.7 mm, R_s = 8−12 Ω/□) were obtained from Delta Technologies, Ltd. Contacts for the electrodes were made from conductive adhesive copper tape (1131, 3M). Sticky-PF was synthesized according to the methodologies that will be reported elsewhere. SWNT films (60 nm thickness, $R_s \sim 70$ Ω/□) were prepared on glass slides with palladium "busbars" as contact layers, using methodologies previously reported (33). The deposition of Sticky-PF was achieved by immersion of the bare SWNT films into a chloroform solution of Sticky-PF for several hours, followed by subsequent soaking of the film in pure chloroform, washing with methanol, and drying with a stream of nitrogen. To minimize contamination from extraneous dust, this procedure was performed in a Class 100 clean room.

2.2. Materials Characterization. The thicknesses of the EC films were controlled by monitoring optical density values at λ_{max} of each polymer film during spraying and were calibrated against directly measured samples using an atomic force microscope (Veeco Innova) with SPMlab Innova software. Electrochemical studies of the polymer films were carried out in a single-compartment three-electrode cell with a platinum flag as the counter electrode, Ag/Ag^+ as the reference electrode or a silver wire as the pseudoreference electrode calibrated using 5 mM Fc/Fc^+ in 0.1 M $LiClO_4$/PC or 0.1 M TBAP/ACN electrolyte solutions, and ITO- or SWNT-film-coated glass slides as working electrodes using an EG&G model PAR273A potentiostat/galvanostat. Spectroelectrochemistry and chronoabsorptometry/chronocoulometry experiments were carried out on a Varian Cary 500 Scan UV−vis−NIR spectrophotometer. Absorbance measurements at λ_{max} were monitored in order to control the optical density of the films with spraying using a Genesys 20 spectrophotometer (Thermo Electron Corp.). Colorimetry was carried out with the use of a Minolta CS-100 Chroma Meter. The samples were illuminated from behind with a D50 (5000 K) light source in a light booth designed to exclude external light. The conductivity of the gel electrolyte was measured using a Fisher Scientific accumet AB30 conductivity meter with a four-cell conductivity probe (cell constant = 1.0 cm^{-1}) calibrated with traceable conductivity standard solutions.

2.3. Assembly of Dual Polymer Window Type Absorption/Transmission ECDs. Two transparent conductive electrode substrates were spray-coated with EC polymer and a PTMA/PMMA blend (actual electroactive area = 2.4 cm^2) of controlled thicknesses. The working electrode with a cathodically coloring PProDOT-$(CH_2OEtHx)_2$ polymer was oxidatively doped, while the counter electrode with NCCP was neutralized prior to device assembly to ensure balance of the charge. The highly transparent and conducting (2.5 mS/cm) gel electrolyte for ECDs was composed of 0.1 M $LiClO_4$, 8.0 wt % of PMMA, and 10 mg of glass beads (Polysciences Inc., 100 μm diameter) per 10 mL of PC/EC (1:1), the latter to maintain a fixed gel electrolyte layer thickness when the device was assembled. All device construction and testing were carried out under ambient conditions. Devices were encapsulated using an extra fast (1−3 min) curable epoxy. Blank devices consisting of two facing ITO- or SWNT-coated glass slides with the gel electrolyte between them, without the electroactive polymer layers, were prepared for all background optical measurements.

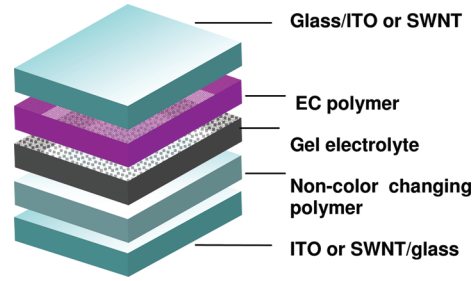

FIGURE 1. Dual polymer absorptive/transmissive window ECD (type B) configuration.

3. RESULTS AND DISCUSSION

3.1. Polymer Combinations in Window ECDs.

A schematic diagram for a dual polymer EC window device utilizing the PProDOT-$(CH_2OEtHx)_2$/non-color-changing polymer combination characterized in this study is shown in Figure 1. The general assembly method for these ECDs utilizes a sandwich-type configuration of two facing transparent electrodes coated with electroactive polymers and separated by an ionically conductive gel electrolyte. The use of a second polymer as an electroactive material for the counter electrode ensures charge balance of the redox reactions taking place on both electrodes and enhances lifetime characteristics by suppressing degradation of the functional material. Two different polymer combinations in window ECDs are discussed below. Type A has both polymers as ECs (cathodically and anodically coloring), while type B combines an EC polymer with a non-color-changing counter-electrode polymer.

3.2. Material Properties. Figure 2 shows a series of UV−vis−NIR absorption spectra of PProDOT-$(CH_2OEtHx)_2$ (with the repeat unit structure shown in the inset) and PTMA polymers at various applied voltages. The polymers were sprayed onto ITO-coated cuvette-size glass slides and cycled between their oxidized and neutral states in a 0.1 M TBAP/ACN electrolyte solution. Cathodically coloring PProDOT-$(CH_2OEtHx)_2$ in its neutral state at −0.20 V (vs Fc/Fc^+ redox couple) exhibits a vibrant magenta color, with the interband π,π^* transition split into a shoulder at 510 nm and two distinct peaks at 550 and 595 nm, attributed to vibronic coupling (34). It is important to note that there is an abrupt decrease in the absorbance of the polymer at wavelengths longer than 600 nm, resulting in a sharp coloration of the

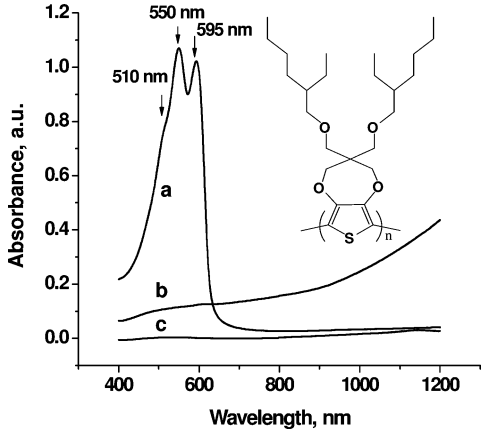

FIGURE 2. Spectra of the spray-cast polymer films on ITO-coated glass slides, electrochemically oxidized and neutralized in a 0.1 M TBAP/ACN electrolyte solution: (a) PProDOT-$(CH_2OEtHx)_2$ in the neutral state at −0.20 V and (b) in the oxidized state at +0.55 V; (c) PTMA in both neutral and oxidized states at −0.10 and 0.70 V, respectively (two overlapping spectra). All potentials are reported versus the Fc/Fc^+ redox couple. The inset shows the repeat unit structure of PProDOT-$(CH_2OEtHx)_2$.

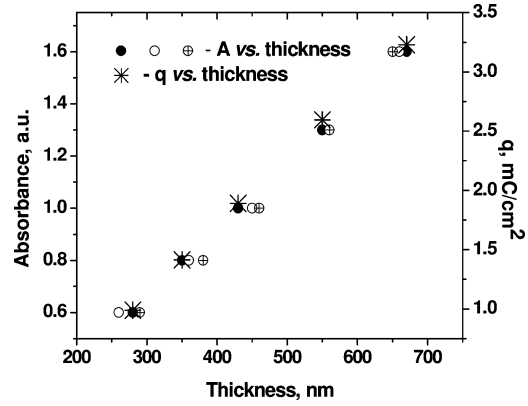

FIGURE 3. Absorbance and charge density as a function of the thickness of PProDOT-$(CH_2OEtHx)_2$ films measured using step-height AFM.

polymer within a small potential window (~200 mV) characteristic of the branched alkyl- and alkoxy-substituted PProDOT derivatives (31). At applied potentials higher than 0.55 V, the polymer is fully oxidized; the π,π^* transition band is fully depleted, while the absorption band at wavelengths >1000 nm associated with bipolaron charge carriers is induced. This process leads to a distinct color change of the film from vibrant magenta to transmissive light blue due to a residual absorbance tail extending from the IR into the visible region. This IR tailing is much lower in absorbance in the case of the PProDOT family of polymers compared to PEDOT, resulting in more complete bleaching of the films, their enhanced transmittance in their clear states, and higher contrast values (21).

The PTMA polymer is transmissive and colorless over the entire UV−visible spectrum with a low absorbance tail in the IR region and demonstrates almost no change in absorbance during the doping/dedoping processes. As shown in Figure 2, the two absorption spectra of the PTMA polymer in its neutral and oxidized states fully overlap with each other (two overlapping dotted lines), demonstrating that this non-color-changing polymer is an excellent candidate for use as an electroactive counter-electrode material in window ECDs (28, 29). As such, it does not add to the absorbance of the ECD in either the absorptive (colored) or bleached state. This allows the device to retain the pure vibrant color of the EC polymer and overcomes transmittance limitations typical for dual EC polymer combinations where the counter-electrode polymer is electrochromically active (i.e., type A polymer combination).

To construct window ECDs with the highest transmittance in the bleached state, a reasonable optical contrast, and a high coloration efficiency coupled with fast redox switching, several device parameters were optimized. Because these characteristics strongly depend on the active layer film thickness, a set of PProDOT-$(CH_2OEtHx)_2$ films were spray-cast onto ITO-coated glass slides. The films had absorbance values ranging from 0.6 to 1.6 measured at 595 nm ($\lambda_{max,2}$). Direct atomic force microscopy (AFM) step-height thickness measurements were performed at least three times for each film. Prior to characterization, the polymer films were electrochemically cycled in a 0.1 M TBAP/ACN solution at a 50 mV/s scan rate until a stable and reproducible redox response had been achieved. The results of optical and electrochemical measurements are presented in Figure 3, demonstrating a linear dependence of the absorbance and charge density with the film thickness.

Table 1 presents the percent transmittance, percent transmittance change, switching time, and composite coloration efficiency values recorded for PProDOT-$(CH_2OEtHx)_2$ between neutral (−0.25 V) and oxidized (0.6 V) states in 10 s time intervals using the tandem chronoabsorptometry/chronocoulometry method and measured at 95% of the full switch at two wavelength absorption maxima for four polymer films. Composite coloration efficiency values (15, 35) (η, cm^2/C) were calculated as the change in the optical density as a function of the charge density required for this change to occur: $\eta = \Delta OD/Q_d$.

Examination of the data shown in Table 1 indicates higher transmittance values in the doped states and faster switching (by a factor of 5) for the thinnest polymer films (films 1 and 2) compared to thicker ones (films 3 and 4), while an overall transmittance contrast (ΔT) reveals the opposite pattern: films 3 and 4 have the largest percent transmittance change values (ΔT = 66.5% and 64.0%, respectively). In general, the optical change of PProDOT-$(CH_2OEtHx)_2$, independent of the film thickness, occurs more rapidly and effectively at a longer wavelength absorption maximum ($\lambda_{max,2}$ = 595 nm) with only a slight (1−2%) difference in transmittance values.

The percent relative luminance (Y) values of the four polymer films were measured colorimetrically as a function of the potential using the CIE 1931 Yxy color space (36, 37). Relative luminance is defined as the transmissivity of the material to visible light calibrated to the sensitivity of the human eye, and, thus, colorimetry provides additional valuable information about the optical properties of EC polymers. When the colorimetry data presented in Figure 4 were examined, films 1 and 2 demonstrated the largest Y param-

Table 1. EC Characteristics at Two Absorption Maxima: $\lambda_{max,1} = 550$ nm and $\lambda_{max,2} = 595$ nm of Four PProDOT-$(CH_2OEtHx)_2$ Films of Varied Thicknesses on ITO-Coated Glass Slides[a]

			$T_{0.95}$, %		$\Delta T_{0.95}$, %		$t_{0.95}$, s		η, cm^2/C	
	thickness, nm	absorbance at $\lambda_{max,2}$, au	$\lambda_{max,1}$	$\lambda_{max,2}$	$\lambda_{max,1}$	$\lambda_{max,2}$	$\lambda_{max,1}$	$\lambda_{max,2}$	$\lambda_{max,1}$	$\lambda_{max,2}$
1	280	0.6	85.0	84.0	58.0	58.5	0.22	0.14	1265	1821
2	360	0.8	74.0	70.0	60.5	59.0	0.37	0.25	840	1215
3	510	1.2	69.0	67.5	66.5	65.5	1.05	0.77	680	835
4	670	1.6	67.0	65.5	64.0	62.0	1.15	1.05	590	700

[a] The optical density of the spray-cast films was controlled by measuring the absorbance at $\lambda_{max,2}$.

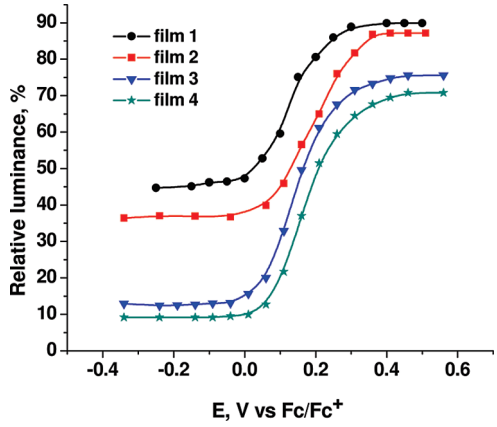

FIGURE 4. Percent relative luminance as a function of the applied potential for PProDOT-$(CH_2OEtHx)_2$ films of different optical densities in a 0.1 M TBAP/ACN electrolyte solution: $A_{film\ 1} = 0.6$ au; $A_{film\ 2} = 0.8$ au; $A_{film\ 3} = 1.2$ au; $A_{film\ 4} = 1.6$ au (at $\lambda_{max,2} = 595$ nm).

eters (89.9% and 87.2%, respectively), although film 2 had a ~5% higher contrast of ΔY than film 1 (45.2% and 50.8%).

Ideal EC materials should have large composite coloration efficiency values (η), which means that a high optical contrast ($\Delta OD = \log T_{0.95\ bleached}/T_{colored}$) is achieved with a small charge injection/extraction. This is especially true for portable ECDs, where power supplies are batteries or supercapacitors and a minimal energy-driven color modulation is required. The coloration efficiency values shown in Table 1 are quite high and comparable with those previously reported for PProDOT-$(CH_2OEtHx)_2$ by our group (31). It is important to emphasize that the thicker polymer films (films 2–4) of PProDOT-$(CH_2OEtHx)_2$ showed a deviation from linear dependence of the peak current values as a function of the scan rate (at 0.01 and 0.2 V/s), indicating the lack of accessibility of redox sites. Cyclic voltammograms of the thicker films measured at fast scan rates have larger peak-to-peak separations compared with those of the thin film 1 ($E_{pa} - E_{pc}$ values ranging from 0.1 to 0.27 V for films 1–4). These results indicate that the process of charge transfer in thicker films is diffusion-limited. Cyclic voltammograms of the thicker films are broader with a larger "capacitive tail", indicating that there is an additional amount of capacitive charging that is a higher fraction of the total charge passed. This charging occurs with no optical change; thus, thicker films would have lower coloration efficiency values. Because the charge density required for the coloration/bleaching of the polymer in fast chronoabsorptmetry/chronocoulometry measurements increases with the film thickness, maximum η characteristics were obtained for the relatively thin films 1 and 2. Taking into account both chronoabsorptometry/chronocoulometry and colorimetry results, film 2 ($A = 0.8$ au at $\lambda_{max,2} = 595$ nm) was chosen as the polymer film with optimal thickness (~360 nm) and optical characteristics required for window ECD fabrication.

A high stability of the constituent polymers upon repetitive redox switching is required to ensure enhanced lifetime characteristics of the devices. For stability measurements, PProDOT-$(CH_2OEtHx)_2$ was sprayed onto an ITO-coated slide and switched between −0.20 and +0.35 V (potential square waves) in 2 s intervals in a 0.1 M TBAP/ACN electrolyte solution. The switching lifetime was measured by recording the evolution of T in the colored and bleached states. The electrochemical cell was refilled with a fresh background solution every 2000 cycles. After 30 000 cycles, an 11% increase in transmittance of the polymer in its neutral state and a 6.3% increase in transmittance of the film in its oxidized state were observed. Overall, the percent transmittance contrast (ΔT) exhibited a relatively small decrease from 69.5% to 64.8%, indicating high stability of the ECP.

Switching studies of the PTMA polymer and its blends with PMMA (the chemical structure of PTMA is shown in the inset of Figure 5a) spray-cast onto ITO-coated slides were performed in a 0.1 M TBAP/ACN electrolyte using cyclic voltammetry. As shown in Figure 5a, a pristine PTMA film exhibited poor electrochemical stability: the peak current density decreases significantly after 20 cycles and ~2.5 times after 100 cycles because of gradual polymer dissolution. Visual observation of the electrode modified with a PTMA film after the experiment indicated partial and non-uniform delamination of the film from the electrode surface.

In order to improve the redox switching stability of the non-color-changing polymer, it was blended with PMMA as a mechanically durable, yet swellable, host ($M_w = 996\ 000$ g/mol) in a 1:4 weight ratio. PTMA/PMMA blends sprayed onto ITO-coated glass slides and air-dried showed a stable behavior upon potential scanning (100 cycles). At the same time, the magnitude of the electroactivity of the polymer blend dropped drastically compared to that of a pristine PTMA film (peak current density decreased by 50%).

It has been previously reported that annealing of polymer blends is a powerful tool to provide interesting morphological changes, leading to a phase-separated structure and, as a result, to an improved interfacial transport and enhanced conductivity (38). The PTMA/PMMA blend film was annealed at 85 °C under a vacuum for 40 min and cooled slowly. This

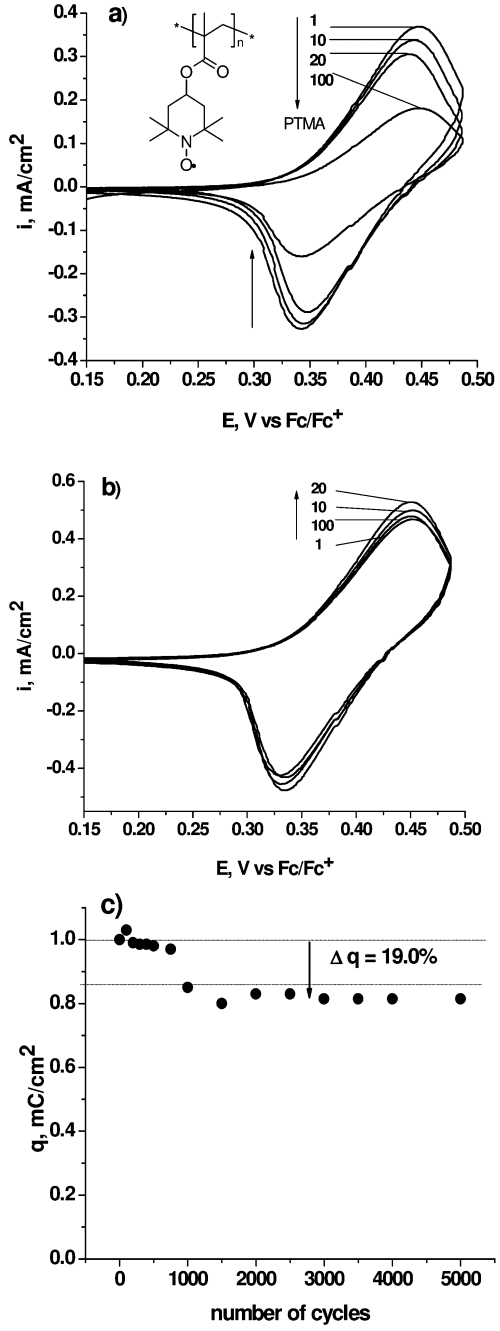

FIGURE 5. Electrochemical stability of PTMA and a PTMA/PMMA blend spray-cast onto ITO-coated glass slides upon repetitive switching (1, 10, 20, and 100 cycles) in the potential range of +0.15 to +0.50 V vs Fc/Fc^+ in a 0.1 M TBAP/ACN electrolyte solution: (a) pristine PTMA; (b) PTMA/PMMA (1:4, w/w) polymer blend annealed at 85 °C for 40 min under a vacuum; (c) charge density vs number of potential steps of the PTMA/PMMA polymer blend annealed at 85 °C for 40 min under a vacuum. The inset in Figure 5a shows the chemical structure of PTMA.

temperature is above the glass transition temperature of the non-color-changing polymer ($T_{g,\ PTMA} = 71$ °C) (24) and was verified as optimal after a series of electrochemical stability experiments and AFM measurements. Annealing of the blend at 120 °C (above $T_{g,\ PMMA} = 105$ °C) caused significant morphological changes, leading to the formation of holes and cracks (39–41).

Figure 5b illustrates the more stable electrochemical behavior (after 100 cycles) of the thin film of PTMA/PMMA sprayed onto ITO-coated glass, annealed at the optimal temperature under a vacuum, and redox-cycled in a 0.1 M TBAP/ACN solution compared to the unannealed PTMA/PMMA film (Figure 5a). It is important to note that the peak current density values became comparable (~0.45 mA/cm^2) to those shown in Figure 5a, demonstrating an enhanced conductivity of the annealed polymer blend due to more ordered morphology. The peak separation of the redox waves is quite narrow (125 mV) for an electroactive polymer, attributable to its fast electrode reaction. Figure 5c demonstrates the long-term stability of the PTMA/PMMA blend film switched by stepping the potential between +0.15 and +0.50 V in 2 s intervals in a 0.1 M TBAP/ACN solution. The electrochemical cell was refilled with a fresh background solution every 1000 cycles. The PTMA/PMMA blend demonstrated a sharp decrease in the charge density between 800 and 1000 redox cycles and, after the cell was refilled with a fresh deoxygenated electrolyte solution, almost no change in the charge from 1000 up to 5000 cycles. These results demonstrate that oxygen may be a contributor to polymer degradation. As will be discussed later, the redox processes become less reversible (the peak separation of the redox waves is 350–400 mV) for thicker PTMA/PMMA films used in device assembly, which could lead to a slower switching and the need for a higher driving voltage during the device operation.

3.3. Dual Polymer Absorptive/Transmissive ECDs on ITO-Coated Glass Electrodes. With the fundamental optical and electrochemical properties of the constituent materials fully characterized, dual polymer absorptive/transmissive window ECDs were assembled as illustrated earlier in Figure 1, composed of glass/ITO/PProDOT-$(CH_2OEtHx)_2$/gel electrolyte/(PTMA/PMMA)/ITO/glass. A PProDOT-$(CH_2OEtHx)_2$ film with an optimal thickness (~360 nm) was used as the EC layer for the working electrode. The PTMA/PMMA polymer blend was annealed at the optimized temperature and utilized as an electroactive layer for the counter electrode. Redox charges of the EC and non-color-changing polymer films were matched prior to device fabrication by stepping the potential between +0.1 and +0.6 V in 0.1 M TBAP/ACN in order to provide a balanced number of redox sites in both polymers and eliminate residual charge formation during operation of the device. During device assembly, the cathodically coloring PProDOT-$(CH_2OEtHx)_2$ film was fully oxidized, while the PTMA/PMMA film was kept in its neutral state. The polymers were both covered with a thin layer of highly conductive (2.5 mS/cm) transparent gel electrolyte and assembled into a sandwich-type configuration.

Spectroelectrochemical studies of the window ECDs were performed to examine the spectral changes during redox switching. Figure 6a presents UV–vis–NIR absorbance spectra of the device as a function of the voltage applied between the working and counter electrodes. At 0.0 V (thick magenta line), the device exhibits the three-component absorption maxima in the visible region characteristic of the EC polymer layer and has a vivid magenta color evident in the photograph in Figure 6b. Upon an incremental increase

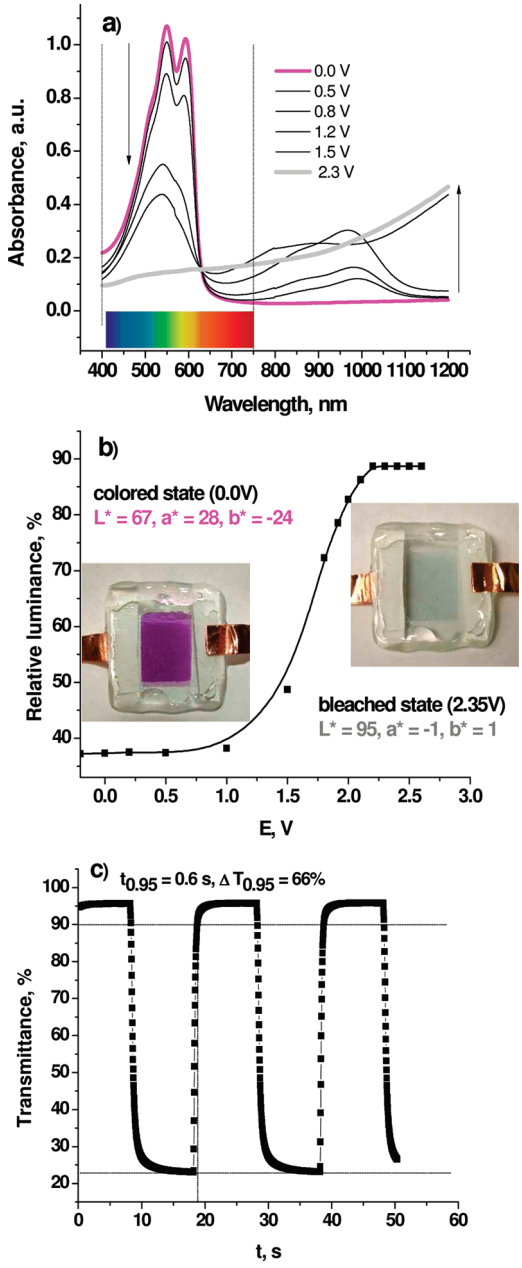

FIGURE 6. Characterization of the dual polymer absorptive/transmissive window device PProDOT-$(CH_2OEtHx)_2$/gel electrolyte/PTMA/PMMA on ITO-coated glass electrodes: (a) spectroelectrochemistry of the device in the fully colored (0.0 V), intermediate (0.8, 1.1, and 1.6 V), and bleached (2.3 V) states; (b) percent relative luminance as a function of the applied potential (insets show photographs of the actual window device; active area = 2.4 cm^2); (c) tandem chronoabsorptometry/chronocoulometry data: redox switching of the device in 10 s interval steps between 0.0 and 2.35 V; percent transmittance reported at the wavelength absorption maximum ($\lambda_{max,2}$ = 596 nm).

of the voltage from 0.0 to 1.2 V, the cathodically coloring polymer oxidizes and a new broad absorption at ~950 nm, attributed to polaron charge carriers, rises in intensity at the expense of the π,π^* transition band. Further oxidation results in the appearance of a new band at wavelengths longer than 1050 nm, corresponding to bipolaron charge carriers (31). The deep magenta color of the device fades into pale-pink hues typical for the intermediate states of the EC polymer film. Finally, when the potential exceeds 2.2 V, PProDOT-$(CH_2OEtHx)_2$ attains its fully doped state (thick gray line); the absorbance between 550 and 600 nm is fully depleted, resulting in a complete bleaching of the device (see the photograph in Figure 6b).

Along with the aforementioned photographs in its extreme states, Figure 6b shows the percent relative luminance change with respect to the applied voltage. The device was a brilliant pure magenta in its colored state (0.0 V) with a relative luminance value of 37%. In its fully oxidized state (2.3 V), it became highly transparent with a light-blue tint and a luminance of 89%, yielding a 52% luminance contrast. The values obtained are almost equal to those of the individual PProDOT-$(CH_2OEtHx)_2$ polymer film with the chosen optimal thickness described earlier (film 2 in Figure 4). The present device was designed especially to give a high level of transmissivity with a luminance of greater than 90%; however, the use of thicker films would allow a deeper color to be attained, as is illustrated in Table 1. In comparison, window-type ECDs utilizing PProDOT-$(CH_2OEtHx)_2$ in combination with the anodically coloring (electrochemically deposited) PBEDOT-NMeCz polymer previously reported by our group (22) also demonstrated a high percent luminance (~93%) in the bleached state. In that device, the EC polymers operated in a complementary manner. As such, both of the polymers contributed to the absorption in the colored state, resulting in larger contrast (~77%) compared to those of the PProDOT-$(CH_2OEtHx)_2$/PTMA devices studied here. At the same time, both of the polymers contributed to the resulting colors of the device in its extreme states. The pure magenta color of the individual PProDOT-$(CH_2OEtHx)_2$ film was inaccessible in the device as the colored state was mixed with the blue color of the oxidized PBEDOT-NMeCz, inducing a new blue-purple hue. More importantly, the neutral PBEDOT-NMeCz is a pale yellow, and combined with the residual absorption of PProDOT-$(CH_2OEtHx)_2$ around 600 nm, the device appeared light green in the bleached state, preventing the device from attaining a colorless bleached state.

For a quantitative description of the color of the window ECDs, a CIE 1976 $L^*a^*b^*$ system has been used. In this system, L^* represents lightness (ranging from 0 to 100), where a^* and b^* are hue and chroma values. Positive and negative a^* values correspond to red and green hues, respectively, while positive and negative b^* are yellow and blue chromas (36, 37). $L^*a^*b^*$ values for the colored and bleached states of the PProDOT-$(CH_2OEtHx)_2$/PTMA window ECD are presented in Figure 6b. During oxidation, the lightness parameter changes from 67 to 95, almost reaching the perfect diffuse white in the color space, while the color changes from magenta with $a^* = 28$ (red hue) and $b^* = -24$ (blue chroma) to nearly colorless $a^* = 1$ and $b^* = -1$.

The simultaneous transmittance change of the device between 0.00 and 2.35 V in 10 s intervals and the charge required for this optical change to occur have been measured, applying a tandem chronoabsorptometry/chronocoulometry technique (Figure 6c). The window device demonstrated a large optical modulation with the percent transmittance at λ_{max} ranging from 23% to 95.5%, reaching very high

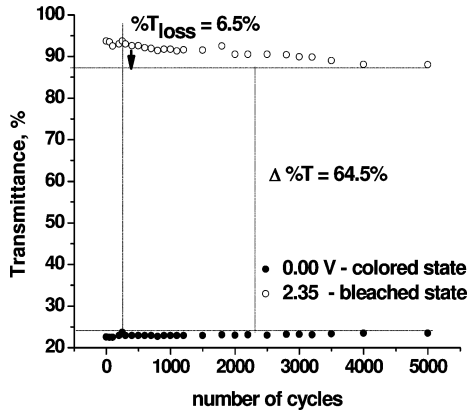

FIGURE 7. EC stability study of the window ECD composed of PProDOT-$(CH_2OEtHx)_2$/gel electrolyte/PTMA/PMMA on ITO-coated glass electrodes. The device was switched with 10 s interval steps between 0.0 and 2.35 V. The percent transmittance is reported at $\lambda_{max,2} = 595$ nm.

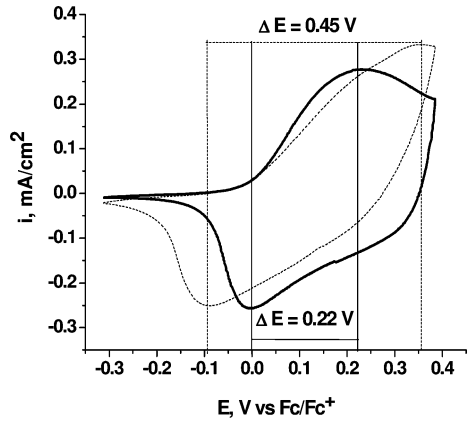

FIGURE 8. Cyclic voltammograms of PProDOT-$(CH_2OEtHx)_2$ in 0.1 M $LiClO_4$/PC, with a scan rate = 50 mV/s: on pristine (dashed line) and Sticky-PF-coated SWNT/glass electrodes (solid line).

transparency in the clear state and exhibiting an impressive (ΔT = 72.6%) transmittance contrast during subsecond switching. A 66% transmittance contrast (calculated for 95% of the full charge/discharge process) was achieved with a 0.6 s switching speed and a 20% transmittance contrast (from 60% to 80%) was achieved at a 160 ms, suggesting that video-type frequencies of 30 Hz for display applications may be achievable with further switching speed optimization.

For stability measurements, the PProDOT-$(CH_2OEtHx)_2$/gel electrolyte/PTMA/PMMA window device was switched between its extreme states with 10 s intervals by stepping the potential from 0.0 to 2.35 V. As shown in Figure 7, this window ECD demonstrated a good stability, gradually losing ~6.5% transmittance in its bleached state with almost no change in T in the colored state. It is important to note that the device was constructed and tested under ambient conditions exemplifying the high stability of our system.

3.4. Dual Polymer Absorptive/Transmissive Devices on SWNT/Glass Electrodes. Next, we investigated and optimized these window-type ECDs using transparent, conductive SWNT films on glass substrates. As stated above, SWNT film electrodes offer several advantages over ITO, especially the viability of transferring this work to flexible plastic substrates allowing repeated bending and rolling. However, the surface characteristics of ITO and SWNTs are fundamentally different. The surface of ITO is polar and hydrophilic and contains metal centers, all characteristics that may aid in wetting by an electroactive material; in contrast, the surface of a SWNT film is nonpolar and hydrophobic and does not contain metal centers whereby heteroatoms may coordinate. Therefore, many organic molecules are prone to delamination.

It is well-known that polycyclic aromatic hydrocarbons, most notably pyrene, form van der Waals interactions with the side walls of SWNTs (42−47). When attached as pendant groups to polymeric backbones, pyrene groups act in concert to form effectively permanent binding between the polymer and the nanotube (48−55). We utilize this strong binding interaction in our design of functionalized polyfluorene (termed Sticky-PF), an alternating copolymer consisting of a fluorene unit substituted with two pyrenes and a fluorene unit substituted with two octyl chains. An ultrathin layer of Sticky-PF on carbon nanotubes effectively changes the surface identity of the SWNTs from a low-energy graphitic lattice to an amorphous lypophilic coating. This coating acts as a "surface primer" wherein organic polymers can better adhere through lypophilic interactions. Furthermore, this coating is thin enough to allow facile charge carrier injection into the electrochemical system.

A comparative study of the electrochemical behavior of PProDOT-$(CH_2OEtHx)_2$ and a PTMA/PMMA blend spray-cast onto pristine and Sticky-PF- and SWNT-coated glass electrodes has been performed by means of cyclic voltammetry. As shown in Figure 8, PProDOT-$(CH_2OEtHx)_2$ polymer deposited on Sticky-PF-and SWNT-coated glass electrodes (solid line) demonstrates a more reversible, less resistive electrochemical response compared to that of the polymer on pristine SWNT (dashed line): the potential difference between anodic and cathodic potential peaks is 2 times lower (ΔE = 0.22 V compared to ΔE = 0.45 V) in the case of the polymer on the Sticky-PF surface-modified electrode. The PTMA/PMMA polymer blend showed a similar behavior.

SWNT electrodes (both pristine and modified with Sticky-PF) were spray-coated with the EC polymer and a PTMA/PMMA blend of the optimal thickness. Window-type ECDs were then assembled in the same fashion as that shown in Figure 1. The optical characteristics of these ECDs on ITO- and SWNT-coated glass electrodes are compared in Table 2. The SWNT-based devices (both pristine and Sticky-PF-coated) were redox-switched with an applied voltage of 2.55 V (comparable to 2.35 V used for ITO-based devices) and demonstrated a high optical contrast of ΔT = 62% and 67% for Sticky-PF-coated SWNT and bare SWNT, respectively. These values are close to the ΔT parameters measured for the ITO-based window devices, although the SWNT-based devices exhibited a lower transmittance in the bleached state and enhanced absorbance in the colored state because of the more absorptive properties of SWNT film substrates in the visible relative to ITO electrodes. Colorimetrically determined color space coordinates for the colored state of the Sticky-PF-coated SWNT window-type ECDs are L^* = 59, a^*

Table 2. Optical Characteristics of the PProDOT-$(CH_2OEtHx)_2$/Gel Electrolyte/PTMA/PMMA Window-Type ECDs on ITO- and SWNT-Coated Glass Electrodes[a]

electrode	voltage, ΔE, V	time, s	$\Delta T_{0.95}$, %	$T_{0.95}$, %	ΔY, %	η, cm^2/C	L^*	a^*	b^*
ITO	2.35	0.6	66	87	51.5	845	**C 67**	**28**	**−24**
							B 95	−1	1
pristine SWNT	2.55	3.4	64	73	63.8	573	**C 51**	**40**	**−39**
							B 92	−2	−3
Sticky-PF-coated SWNT	2.55	2.4	62	74	64.5	669	**C 59**	**40**	**−36**
							B 92	−2	−4
Sticky-PF-coated SWNT	3.5	0.27	44	80	40	750			

[a] $L^*a^*b^*$ values are indicated for the colored (**C**) and bleached (B) states of devices.

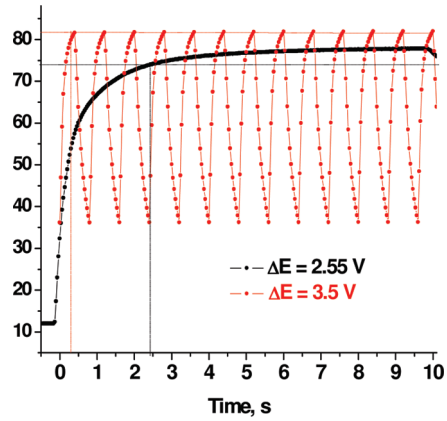

FIGURE 9. Potential switching steps of the PProDOT-$(CH_2OEtHx)_2$/gel electrolyte/PTMA/PMMA device on Sticky-PF-coated SWNT-coated glass electrodes: (black) from −0.2 to +2.35 V (2.55 V voltage difference); (red) from −0.9 to +2.6 V (3.5 V voltage difference). The percent transmittance is reported at $\lambda_{max,2}$ = 596 nm.

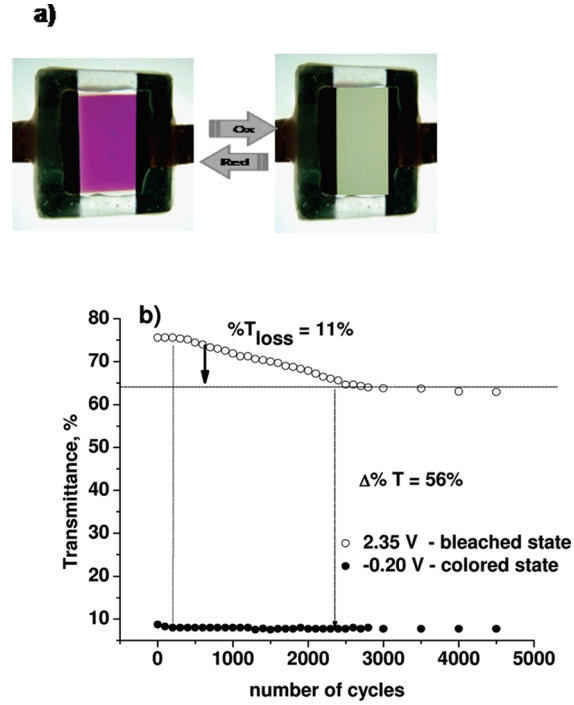

FIGURE 10. (a) Photographs of the window-type ECD PProDOT-$(CH_2OEtHx)_2$/gel electrolyte/PTMA/PMMA on Sticky-PF-coated SWNT-coated glass electrodes in the two extreme states. (b) EC stability of the device switched with 10 s interval steps between −0.20 and +2.35 V. The percent transmittance is reported at $\lambda_{max,2}$ = 596 nm.

= 40, and $b^* = -36$, which are indicative of a more intense deep-purple color compared to the previously described magenta-colored ITO-based devices (Figure 6b). Upon oxidation, the SWNT-based device bleaches to a high extent, exhibiting $L^* = 92$, $a^* = 2$, and $b^* = -4$.

An enhanced switching speed (with nearly identical optical changes) was observed for the SWNT films coated with Sticky-PF compared to pristine SWNT films, confirming an improved electroactivity of the polymers on SWNTs coated with a "sticky" layer. Additionally, the larger η value of the Sticky-PF-coated SWNT device results from the smaller charge required for the optical modulation (because ΔT parameters are similar for both modified and pristine SWNT devices), indicating a more efficient redox switching, possibly because of more facile charge injection characteristics.

In general, compared to ITO-based devices, window-type ECDs on SWNT electrodes switch 4−5 times slower, presumably because of the higher sheet resistance of the latter. In order to overcome this disadvantage, different voltages have been applied to the devices to probe the switching speed characteristics. Figure 9 illustrates the influence of the applied voltage on the switching speed and single-wavelength measurements of the ΔT's of the Sticky-PF-coated SWNT-based window-type ECDs. The device in Figure 9 (black curve) was redox-switched between the colored and clear states with a 2.55 V overall voltage (from −0.2 to +2.35 V) in 10 s intervals, attaining a high percent transmittance contrast of 68% in 2.4 s. Increasing the switching voltage up to 3.5 V (from −0.9 to +2.6 V) (Figure 9, red curve) allowed a significantly faster device performance, with a reasonable optical contrast of 43% achieved within 0.27 s.

For stability measurements, the PProDOT-$(CH_2OEtHx)_2$/gel electrolyte/PTMA/PMMA window-type device on Sticky-PF-coated SWNT-coated glass electrodes was switched between its extreme states with 10 s interval steps by stepping the potential from −0.20 to +2.35 V (Figure 10). The SWNT-based window ECDs showed a similar trend compared to the ITO-based devices: it demonstrated an 11.0% loss in optical contrast due to a decrease in transmittance in the bleached state with stabilization after 2500 cycles. As such, we believe that this loss of transmittance is due to the inability to access all of the polymer, and small regions of the reduced polymer remain with repeated switching, ultimately reaching a limiting value.

4. CONCLUSIONS

This paper describes the construction and characterization of dual polymer absorptive/transmissive window-type ECDs on ITO- and SWNT-coated glass electrodes using an EC/non-color-changing polymer combination. Judicious utilization of the non-color-changing and fully transparent PTMA/PMMA blend, in combination with the cathodically coloring PProDOT-$(CH_2OEtHx)_2$ polymer of optimal film thickness, resulted in highly performing ECDs based on the parameters of a high transmittance (>95% for ITO-based devices and 78% for SWNT-based devices) with little or no residual color, a high optical contrast, and retention of the pure vibrant magenta color exhibited by the color-active polymer. The fast switching (0.1−1.0 s) and high stability (thousands of double potential steps) of the devices suggests their utility in broad-band EC applications including highly transmissive smart vision systems and rapidly operating EC displays. The promising results obtained for the Sticky-PF-coated SWNT-based devices open a pathway toward flexible ECDs.

Acknowledgment. The authors gratefully acknowledge Ciba (a part of BASF) and Nanoholdings LLC for funding of this research.

REFERENCES AND NOTES

(1) Heuer, H. W.; Wehrmann, R.; Kirchmeyer, S. *Adv. Funct. Mater.* **2002**, *12*, 89–94.
(2) DuBois, C. J.; Abboud, K. A.; Reynolds, J. R. *J. Phys. Chem. B* **2004**, *108*, 8550–8557.
(3) Argun, A. A.; Cirpan, A.; Reynolds, J. R. *Adv. Mater.* **2003**, *15*, 1338–1341.
(4) Beaupre, S.; Dumas, J.; Leclerc, M. *Chem. Mater.* **2006**, *18*, 4011–4018.
(5) Monk, P. M. S.; Delage, F.; Costa Vieira, S. M. *Electrochim. Acta* **2001**, *46*, 2195–2202.
(6) Corr, D.; Stobie, N.; Bach, U.; Fay, D.; Kinsella, M.; McAtamney, C.; O'Reilly, F.; Rao, S. N. *Solid State Ionics* **2003**, *165*, 315–321.
(7) Monk, P. M. S. In *Handbook of Luminescence, Display Materials, and Devices*; Nalwa, H. S., Rohwer, L. S., Eds.; American Scientific Publishers: Valencia, CA, 2003; Chapter *3*, p 261.
(8) Monk, P. M. S.; Mortimer, R. J.; Rosseinsky, D. R. *Electrochromism: Fundamentals and Applications*; VCH: Weinheim, Germany, 1995.
(9) Granqvist, C. G. *Electrochim. Acta* **1999**, *44*, 2983–2991.
(10) Rauh, R. D. *Electrochim. Acta* **1999**, *44*, 3165–3176.
(11) De Tacconi, N. R.; Rajeshwar, K.; Lezna, R. O. *Chem. Mater.* **2003**, *15*, 3046–3062.
(12) Somani, P. R.; Radhakrishnan, S. *Mater. Chem. Phys.* **2003**, *77*, 117–133.
(13) Mortimer, R. J. *Electrochim. Acta* **1999**, *44*, 2971–2981.
(14) De Paoli, M. A.; Nogueira, A. F.; Machado, D. A.; Longo, C. *Electrochim. Acta* **2001**, *46*, 4243–4249.
(15) Argun, A. A.; Aubert, P.-H.; Thompson, B. C.; Schwendeman, I.; Gaupp, C. L.; Hwang, J.; Pinto, N. J.; Tanner, D. B.; MacDiarmid, A. G.; Reynolds, J. R. *Chem. Mater.* **2004**, *16*, 4401–4412.
(16) Sonmez, G.; Shen, C. K. F.; Rubin, Y.; Wudl, F. *Angew. Chem., Int. Ed.* **2004**, *43*, 1498–1502.
(17) Beaujuge, P. M.; Ellinger, S.; Reynolds, J. R. *Adv. Mater.* **2008**, *20*, 2772–2776.
(18) Gunbas, G. E.; Durmus, A.; Toppare, L. *Adv. Funct. Mater.* **2008**, *18*, 2026–2030.
(19) Dyer, A. L.; Reynolds J. R. In *Handbook of conducting polymers: Theory, Synthesis, Properties, and Characterization*; Skotheim, T. A., Reynolds, J. R., Eds.; CRC Press: Boca Raton, FL, 2007; p 20.
(20) Padilla, J.; Otero, T. F. *Electrochem. Commun.* **2008**, *10*, 1–6.
(21) Schwendeman, I.; Hickman, R.; Sonmez, G.; Schottland, P.; Zong, K.; Welsh, D. M.; Reynolds, J. R. *Chem. Mater.* **2002**, *14*, 3118–3122.
(22) Cirpan, A.; Argun, A. A.; Grenier, C. R. G.; Reeves, B. D.; Reynolds, J. R. *J. Mater. Chem.* **2003**, *13*, 2422–2428.
(23) Nakahara, K.; Iwasa, S.; Satoh, M.; Morioka, Y.; Iriyama, J.; Suguro, M. *Chem. Phys. Lett.* **2002**, *359*, 351–354.
(24) Nishide, H.; Iwasa, S.; Pu, Y.-J.; Suga, T.; Nakahara, K.; Satoh, M. *Electrochim. Acta* **2004**, *50*, 827–831.
(25) Nishide, H.; Suga, T. *Electrochem. Soc. Interface* **2005**, *14*, 32–36.
(26) Suga, T.; Konishi, H.; Nishide, H. *Chem. Commun.* **2007**, 1730–1732.
(27) Oyaizu, K.; Ando, Y.; Konishi, H.; Nishide, H. *J. Am. Chem. Soc.* **2008**, *130*, 14459–14461.
(28) Takahashi, Y.; Oyaizu, K.; Honda, K.; Nishide, H. *J. Photopolym. Sci. Technol.* **2007**, *20*, 29–34.
(29) Takahashi, Y.; Oyaizu, K.; Honda, K.; Nishide, H. *Polym. J.* **2008**, *20*, 763–767.
(30) Welsh, D. M.; Kumar, A.; Morvant, M. C.; Reynolds, J. R. *Synth. Met.* **1999**, *102*, 967–968.
(31) Reeves, B. D.; Grenier, C. R. G.; Argun, A. A.; Cirpan, A.; McCarley, T. D.; Reynolds, J. R. *Macromolecules* **2004**, *37*, 7559–7569.
(32) Reeves, B. D.; Unur, E.; Ananthakrishnan, N.; Reynolds, J. R. *Macromolecules* **2007**, *40*, 5344–5352.
(33) Wu, Z.; Chen, Z.; Du, X.; Logan, J. M.; Sippel, J.; Nikolou, M.; Kamaras, K.; Reynolds, J. R.; Tanner, D. B.; Hebard, A. F.; Rinzler, A. G. *Science* **2004**, *305*, 1273–1277.
(34) Kumar, A.; Welsh, D. M.; Morvant, M. C.; Piroux, F.; Abboud, K. A.; Reynolds, J. R. *Chem. Mater.* **1998**, *10*, 896–902.
(35) Gaupp, C. L.; Welsh, D. M.; Rauh, R. D.; Reynolds, J. R. *Chem. Mater.* **2002**, *14*, 3964–3970.
(36) Berns, R. S. *Billmeyer and Saltzman's Principles of Color Technology*, 3rd ed.; John Wiley & Sons, Inc.: New York, 2000.
(37) *CIE Technical Report: Colorimetry*, 3rd ed.; Commission Internationale De L'eclairage: Vienna, Austria, 2004.
(38) De Paoli, M.-A.; Gazotti, W. A. *Macromol. Symp.* **2002**, *189*, 83–103.
(39) Iyengar, N. A.; Harrison, B.; Duran, R. S.; Shanze, K. S.; Reynolds, J. R. *Macromolecules* **2003**, *36*, 8978–8985.
(40) Buschbaum, P. M.; Stamm, M. *Macromolecules* **1998**, *31*, 3686–3692.
(41) Affrossman, S.; O'Neill, S. A.; Stamm, M. *Macromolecules* **1998**, *31*, 6280–6288.
(42) Chen, R. J.; Zhang, Y.; Wang, D.; Dai, H. *J. Am. Chem. Soc.* **2001**, *123*, 3838–3839.
(43) Nakashima, N.; Okuzono, S.; Tomonari, Y.; Murakami, H. *Proc. Electrochem. Soc.* **2003**, *15*, 277–284.
(44) Gomez, F. J.; Chen, R. J.; Wang, D.; Waymouth, R. M.; Dai, H. *Chem. Commun.* **2003**, 190–191.
(45) Rahman, G. M. A.; Guldi, D. M.; Cagnoli, R.; Mucci, A.; Schenetti, L.; Vaccari, L.; Prato, M. *J. Am. Chem. Soc.* **2005**, *127*, 10051–10057.
(46) Campidelli, S.; Klumpp, C.; Bianco, A.; Guldi, D. M.; Prato, M. *J. Phys. Org. Chem.* **2006**, *19*, 531–539.
(47) Lim, H.; Shin, H. S.; Shin, H.-J.; Choi, H. C. *J. Am. Chem. Soc.* **2008**, *130*, 2160–2161.
(48) Tang, B. Z.; Xu, H. *Macromolecules* **1999**, *32*, 2569–2576.
(49) Lou, X.; Daussin, R.; Cuenot, S.; Duwez, A. S.; Pagnoulle, C.; Detrembleur, C.; Bailly, C.; Jerome, R. *Chem. Mater.* **2004**, *16*, 4005–4011.
(50) Wu, X.; Shi, G. *J. Mater. Chem.* **2005**, *15*, 1833–1837.
(51) Wang, D.; Ji, W.-X.; Li, Z.-C.; Chen, L. *J. Am. Chem. Soc.* **2006**, *128*, 6556–6557.
(52) Bahun, G. J.; Wang, C.; Adronov, A. *J. Polym. Sci., Part A: Polym. Chem.* **2006**, *44*, 1941–1951.
(53) Yuan, W. Z.; Sun, J. Z.; Dong, Y. Q.; Haussler, M.; Yang, F.; Xu, H. P.; Qin, A. J.; Lam, J. W. Y.; Zheng, Q.; Tang, B. Z. *Macromolecules* **2006**, *39*, 8011–8020.
(54) Yuan, Z.; Mao, Y.; Zhao, H.; Sun, J. Z.; Xu, H. P.; Jin, J. K.; Zheng, Q.; Tang, B. Z. *Macromolecules* **2008**, *41*, 701–707.
(55) Yuan, W. Z.; Sun, J. Z.; Liu, J. Z.; Dong, Y.; Li, Z.; Xu, H. P.; Qin, A.; Haussler, M.; Jin, J. K.; Zheng, Q.; Tang, B. Z. *J. Phys. Chem. B* **2008**, *112*, 8896–8905.

AM900435J